Solid State Ionics 232 (2013) 44–48

Contents lists available at SciVerse ScienceDirect

Solid State Ionics

journal homepage: www.elsevier.com/locate/ssi

A high temperature operating nanofibrous polyimide separator in Li-ion battery

Wen Jiang, Zhihong Liu *, Qingshan Kong, Jianhua Yao, Chuanjian Zhang, Pengxian Han, Guanglei Cui *

Qingdao Institute of Bioenergy and Bioprocess Technology, Chinese Academy of Sciences, 266101 Qingdao, P.R. China

ARTICLE INFO

Article history:
Received 27 August 2012
Received in revised form 28 October 2012
Accepted 6 November 2012
Available online 23 December 2012

Keywords:
Thermosetting polyimide
Separator
Electrospinning
High temperature

ABSTRACT

Separators possessing thermal stability are highly desired to meet the requirement of application in high power lithium batteries. In this paper, the thermosetting polyimide (PI) nano-fibers based nonwoven separators have been developed by electrospining technique and followed by thermal imidization and mechanical pressing with improved thermal stability and considerable mechanical strength. The high concentration of tortuous nanopores structure and intrinsic chemical configuration lead to good ionic transport and improved electrolyte wettability. The electrochemical characterization at high temperature of 120 °C demonstrates that the LiBOB/PC soaked polyimide nonwovens is an excellent electrolyte system for high temperature operation owing to possessing high oxidative potential, excellent lithium deposition-stripping performance and considerable ionic conductivity. The cells using LiBOB/PC soaked polyimide nonwovens as separator still exhibit stable charge–discharge profiles with quantitative coulumbic efficiency and satisfactory cyclability at 120 °C. The superior electrochemical performance at high temperature could endow these polyimide nonwovens promising alternative to PP separators for high power or high temperature application with superior safety characteristic.

1. Introduction

In lithium-ion batteries, the separator plays a key role in separating the positive and negative electrodes to prevent electrical short circuit. Polyolefin microporous membranes such as polyethylene (PE) and polypropylene (PP) have been commercially available as major separators for the lithium ion battery [1–5]. However, these polyolefin-based separators suffer from a poor thermal shrinkage at relatively high temperature above 90 °C [6–15], which has raised serious concern over their ability to prevent internal electrical short circuit at these high temperature conditions. Although polyolefin membranes have a function of thermal shut-down at a specific temperature for safety, they cannot bear this temperature for a long time, and will melt once the temperature becomes higher. So the battery safety problems hinder their future application in high power devices such as electric vehicles, hybrid electric vehicles and robots [16,17].

In addition, batteries operating at relatively high temperature are needed for some specific application, such as Measurement While Drilling (MWD) tools for the oil drilling market. The development of secondary lithium batteries capable of operation in relatively high temperature range, represent an interesting alternative to state-of-the-art battery technology [18]. Some separators and polymeric electrolytes was claimed to be able to perform in relatively higher temperature battery [19–22]. However, their electrochemical performance was studied only in the $LiPF_6$ based electrolyte at ambient temperature, not really tested in the lithium bis(oxalate) borate (LiBOB) based electrolyte at high temperature. Very recently, Palacin et al. explored two sheets of Whattman GF/d borosilicate glass fiber (675 μm thich) as real high temperature separator [18]. This inorganic glass fiber separator was too thick and heavy, which definitely resulted in poor rate capability and lower energy density. Therefore, it is urgent to develop thin and light organic separator which can really meet the requirement of high temperature electrochemical stability.

Thermosetting polyimides are known for thermal stability, good chemical resistance and excellent mechanical properties, which are sufficient for a torture of continuous use at temperatures of 230 °C and for short excursions as high as 480 °C. Polyimides are also inherently resistant to flame combustion, which endow PI based separators with unique thermal stability [22,23]. However, the electrochemical performance of nanofibrous polyimide separator was explored using the $LiPF_6$/EC/EMC electrolyte at ambient temperature in our previous report [22]. The high temperature electrochemical performance of nanofibrous PI separator was not really disclosed yet. In this regard, the high temperature electrochemical properties of nanofibrous PI nonwovens were further investigated in LiBOB/PC electrolyte at elevated temperature, which would provide valuable insight into the high temperature characteristics for high power devices such as electric vehicles or Measurement While Drilling (MWD) tools.

2. Experimental

2.1. Materials and measurements

N, N-dimethylacetamide (DMAc, 99.5%, Tianjin Fuyu Chem. Co.), pyromellitic dianhydride (PDA, ≥98.5%, Sinopharm. Chemical Reagent

* Corresponding authors. Tel.: +86 532 80662746; fax: +86 532 80662744.
E-mail addresses: liuzh@qibebt.ac.cn (Z. Liu), cuigl@qibebt.ac.cn (G. Cui).

0167-2738/$ – see front matter © 2012 Elsevier B.V. All rights reserved.
http://dx.doi.org/10.1016/j.ssi.2012.11.010

Co.) and 4,4'-diaminophenyl ether (ODA, 98%, Alfa Aesar) were commercially available and used without further purification. Lithium bis(oxalate)borate (LiBOB, ≥99%, Suzhou Fosai Co., Ltd.), propylene carbonate (PC, Shenzhen Capchem Technology Co., Ltd.), $LiFePO_4$ (Tianjin Strain Energy Science and Technology Ltd., particle size: 3 ± 1.0 μm, carbon content: 1.5–2.0%) and PP separator (Celgard 2500, USA) were purchased as battery grade.

Inherent viscosity is directly related relative molecular weight of a polymer. Inherent viscosity of PI precursor PDA-ODA was measured using an Ubbelohole Viscometer (Φ 0.8–0.9 mm) in DMAc at 25 °C. IR spectra of PI precursor PDA-ODA and PI nano fibers samples were recorded on a Nicolet iN10 spectrophotometer.

2.2. Electrospinning and preparation of PI nanofiber nonwovens

The typical polymerization of PI precursor was reported previously [24] and described as follows. Equimolar amounts of PDA (4.3624 g, 0.02 mol) and ODA (4.0048 g, 0.02 mol) and 30.6 g solvent DMAc were mixed in a 250 mL four-necked flask equipped with a mechanical stirrer under argon atmosphere at 0 °C for 24 hrs to give the highly sticky poly(amide acid) solution (20%, w/w). The synthesis of polyimide and its precursor is shown in Scheme S1. The inherent viscosity of the polymer product was measured to be 2.11 dLg^{-1} by diluting the as-synthesized highly sticky solution into diluted DMAc solution. The as-synthesized sticky PI precursor PDA-ODA solution was kept in a refrigerator for later electrospinning use.

The electrospinning process was performed by using the above precursor solution in DMAc. The electrospinning equipments comprise a high voltage power supply (Spellman SL150, USA), a syringe pump (New Era Pump system NE-1600, USA) and a rotating collector with the diameter of 10 cm. The inner diameter of the spinneret is 0.9 mm and the speed of the solution supply is 0.2 mL per hour. A 25 kV electrical potential is applied to a 25 cm distance between the spinneret and the collector. The as-electrospun PDA-ODA nanofibers were collected in a form of nonwoven sheets on the aluminium foil at the cylindrical surface of collector. The imidization of nanofiber sheets from PDA-ODA to PI was carried out in an oven by the following steps: (i) heating up to 100 °C for 30 min to remove the residue solvent; (ii) heating up to 200 °C and held for 30 min; (iii) heating up to 300 °C and held for 30 min.

After thermal imidization, the nonwoven mats were mechanically pressed on a preforming machine (769YP-24B, Tianjin) under different oil pressure for 3 min. The samples under oil pressure of 1 MPa, 2 MPa, 3 MPa and 5 MPa are referred as PI-1, PI-2, PI-3 and PI-5, respectively. The whole process was illustrated in Scheme S2.

2.3. Characterization of the PI nonwovens

The microporous morphology, air permeability, thermal shrinkage and mechanical strength of separators are the major characteristics that should be carefully monitored. The surface morphologies of separators were examined using a field emission scanning electron microscope (Hitachi S-4800). The air permeability was examined with a Gurley densometer (4110N, Gurley) by measuring the time necessary for air to pass through a determined volume under a given pressure. The air permeability represented by the Gurley value (sec 100 cc^{-1}) was considered to be a useful benchmark that quantitatively reflects the microporous structure of a separator. The mechanical properties were measured using an Inston-3300 universal testing machine (USA) at a stretching speed of 1.66 mm sec^{-1} with the straps of about 1 cm wide and 5 cm long.

Liquid electrolyte uptakes of the separators were measured by immersing the nonwovens in the liquid electrolyte (0.5 M LiBOB/PC) for 2 hrs"". Liquid electrolyte-soaked membranes were weighed quickly after removing the excrescent surface solution using wipes. The electrolyte uptake (EU) was calculated by the equation: $EU\ (\%) = (W_1 - W_0)/W_0 \times 100\%$, where W_1 and W_0 are the weights of the electrolyte-soaked membranes and dry membranes, respectively.

The porosity of the separators was determined using n-butanol uptake. For this purpose, the mass of the separators was measured before and after immersion in n-butanol for 2 hrs. The porosity of the membrane was calculated using the equation: $porosity = (m_b/\rho_b)/(m_b/\rho_b + m_p/\rho_p) \times 100\%$, where m_b and m_p are the mass of n-butanol and the separator, ρ_b and ρ_p are the density of n-butanol and the polymer, respectively.

The thermal shrinkage of the separators was determined by measuring their dimension change after they were subjected to heat treatment in an oven at temperature of 150 °C for 1 h.

2.4. High temperature electrochemical characterization of PI nonwovens

Thanks to the highly stability and superior electrochemical performance of LiBOB/PC electrolyte at high temperature [25–27], The performance of PI nonwoven at high temperature of 120 °C was characterized

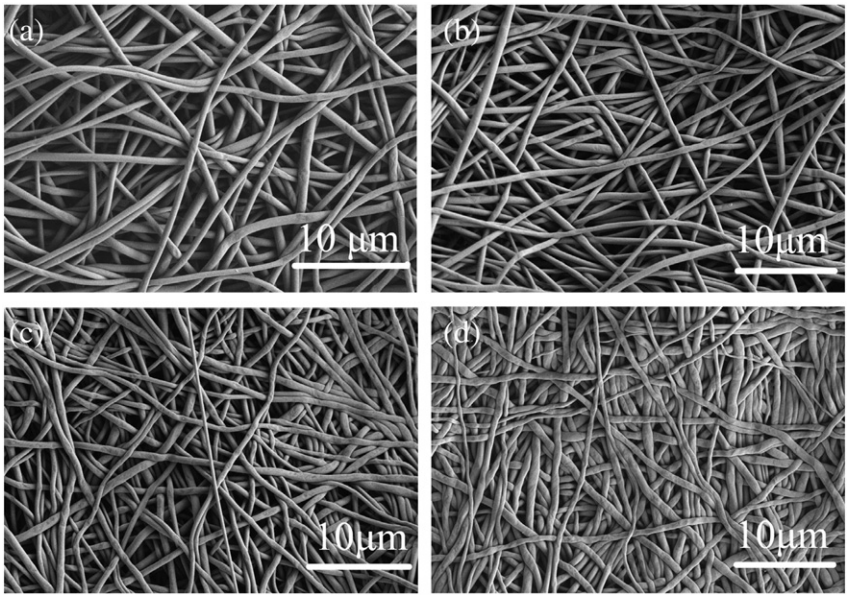

Fig. 1. Typical SEM images of PI nanofibers nonwovens after mechanical pressing: (a) PI-1, (b) PI-2, (c) PI-3 and (d) PI-5.

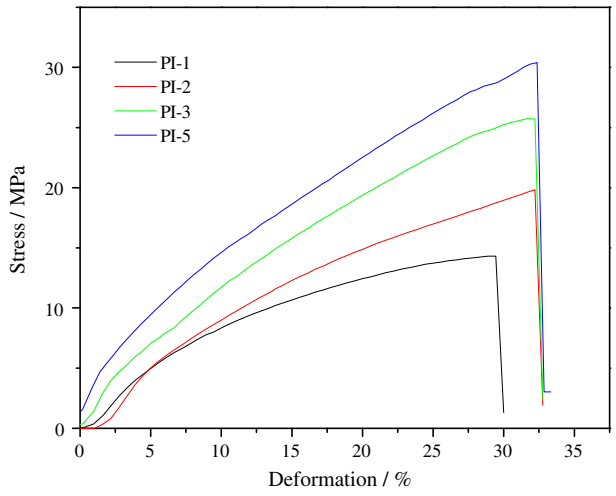

Fig. 2. The stress–deformation curves of the PI nonwovens.

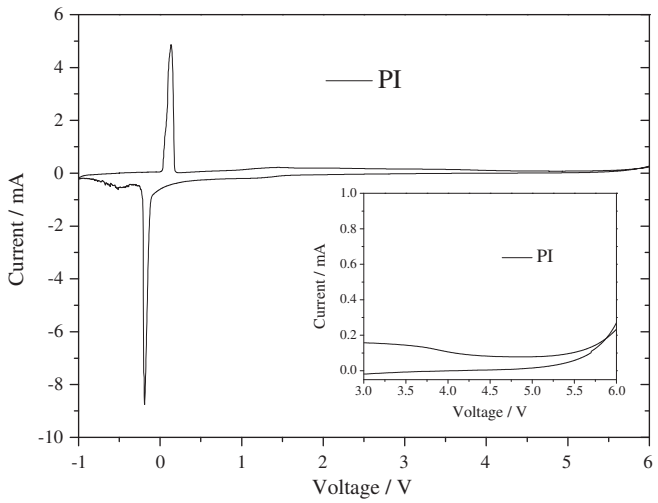

Fig. 4. Linear sweep voltammograms of a liquid electrolyte-soaked PI-5 nonwoven at 120 °C.

in a 0.5 M LiBOB/PC liquid electrolyte. The electrochemical stability window of the liquid electrolyte soaked separators was evaluated by a linear sweep voltammetry experiment performed on a working electrode of stainless-steel and a counter electrode of lithium metal at a scan rate of 1.0 mV s^{-1}. The ionic conductivity of the liquid electrolyte-soaked separator between two stainless-steel plate electrodes was obtained by an AC impedance analysis using a Zahner Zennium electrochemical working station over a frequency range of 1 Hz to 10^6 Hz.

A coil cell (2032-type) was assembled by sandwiching a separator between a lithium metal foil anode and a $LiFePO_4$ cathode and then filling liquid electrolyte. The $LiFePO_4$ electrode was prepared by a doctor-blading and the mass ratio of $LiFePO_4$/carbon black/PVdF was 0.8/0.1/0.1 (w/w/w). All assembly of cells was carried out in an argon-filled glove box. The charge/discharge curves and cycle performance of cells were examined using a LAND battery testing system at 120 °C. The cells were cycled at a fixed charge/discharge current density of 0.5 C (62 mA g^{-1})/0.5 C (62 mA g^{-1}) for cycle life testing under a voltage range between 2.5 V and 4.0 V.

3. Results and discussion

3.1. Characterization of the nonwoven separators

Infrared (IR) spectra of the precursor PDA-ODA and PI nanofibers are presented in Fig. S1. After curing reaction at 300 °C, the broad absorption band between 3700 and 2000 cm^{-1} ascribed to the stretching vibration absorption of N—H and O—H drops drastically and the strong absorption band between 1700 and 1600 cm^{-1} assigned to the stretching vibration absorption of CO—NH and COOH disappears. The absorption bands between 1800 and 750 cm^{-1} becomes well resolved. Among them, the sharp absorption peaks at 1770 and 1720 cm^{-1} are related to the stretching vibration absorption of C O in the imide structure. The aforementioned IR spectra variation confirms that the nanofibrous PDA-ODA was imidized into nanofibrous PI completely. The PI nonwovens obtained by quantitative imidization would have a better chemical and thermal stability.

It is observed from SEM images in Fig. 1 that the fibers are randomly arranged with a diameter size of around 500 nm. Generally, the electrospun nonwovens still suffer from large-sized pores and poor mechanical tensile strength [28,29]. In our case, the as-electrospun PI nonwovens underwent high mechanical pressing from 1 MPa to 5 MPa for 3 min in order to obtain smaller pore size and higher mechanical strength. From the SEM images of Fig. 1, we can observe the pressed morphology of the PI nonwovens with well-connected interstitial voids. After being pressed, the PI nonwovens became compressed with diminished pore size (mostly below 1.0 μm for PI-5). These tortuous, not straightforward small pores and uniform pore distribution are well qualified for better performance in lithium ion battery.

The mechanical strength test results of the PI nonwovens are presented in Fig. 2. With increasing pressure of the pressing treatment from 1 MPa to 5 MPa, the tensile strength of PI nonwovens were raised from 12 MPa to 31 MPa with deformation of about 30%, which is attributed to the stronger physical bonding between the nanofibers. Their tensile strength was isotropic owing to the random arrangement of nanofibers corroborated by SEM observation. The

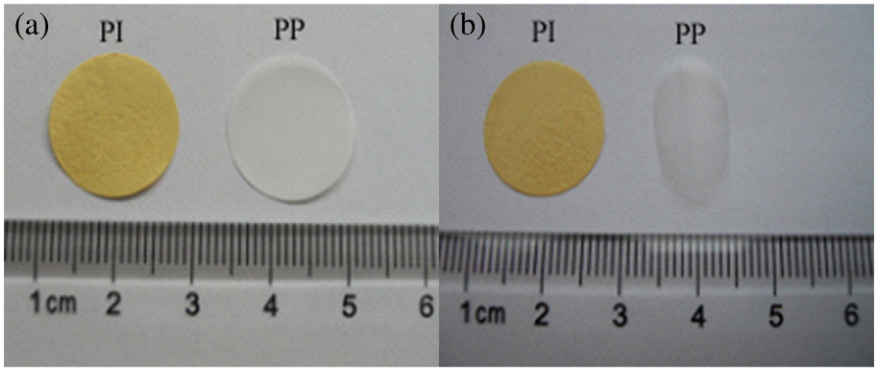

Fig. 3. The photographs of the PP membrane and PI nonwoven before (a) and after (b) thermal treatment at 150 °C for 1 h.

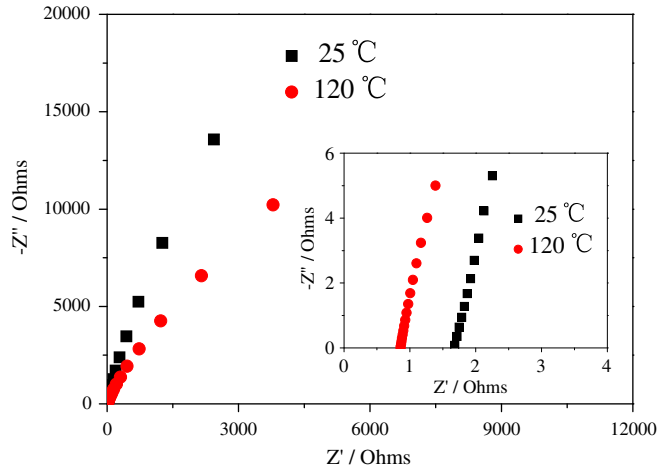

Fig. 5. Nyquist plots of the cells SS/ liquid electrolyte-soaked PI-5 nonwoven /SS at 25 °C and 120 °C, respectively.

unoptimized value of 31 MPa is lower than that of the machine direction strength (140 MPa, seen in Fig. S2(a)) of uniaxially stretching PP membrane, but this is double that of its transverse direction strength (15 MPa, seen in Fig. S2(b)). In regards of safety in electrode sheets stacking during battery assembly or accident collision, these PI nonwoven separators provide more reliable mechanical property.

The thickness, electrolyte uptake, porosity and air permeability of PI nonwovens and the reference Celgard membrane are listed in Table S1. Compared to the commercialized microporous PP separator, the PI nonwovens possess higher porosity ranging from 73% to 87%, extremely lower Gurley value ranging from 2.1 s to 7.5 s and higher electrolyte uptake ranging from 27% to 340%. It was shown in Fig. S3 that the PI nonwoven was quickly wetted by the liquid electrolyte. This improvement in the electrolyte wettability is attributed to the relatively polar constituent of imide structure and also the nano porous structure [24].

The thermal shrinkage of separators is another important factor that influences the battery safety. The photographs of the PI nonwovens and Celgard PP membrane before and after thermal treatment at 150 °C for an hour are presented in Fig. 3. It can be seen that the Celgard PP membrane shrank 35% at the machine direction after heating, while the PI nonwoven did not shrink at all. From viewpoint of thermal stability, the thermosetting PI does not melt under 300 °C, while PP melts at around 160 °C (seen in Fig. S4). The serious shrinkage of uniaxially stretched PP separator was originated from the internal stress formed historically during the stretching and cooling stage. The transverse direction of PP membrane did not shrink because of no stretching in this direction. In addition, PI possesses self-extinguished property and cannot catch a fire. So, PI nonwovens are anticipated to work as separators in lithium ion battery with enhanced thermal safety and fireproof performance compared to the commercialized PP membranes.

3.2. Electrochemical stability of the PI nonwoven separator at high temperature

The electrochemical stability of the liquid electrolyte-soaked PI nonwoven plays a crucial role in maintaining the long-term reversibility of cell chemistry. From Fig. 4, it could be seen that liquid electrolyte-soaked PI-5 nonwoven started to oxidatively decompose above 4.5 V vs Li^+/Li at 120 °C. The electrochemical stability above 4.5 V could endow this PI nonwoven for a high voltage battery application even at elevated temperature at 120 °C The cathodic current onset was observed to be about −0.2 V vs Li^+/Li, which was corresponding to the electrochemical deposition of lithium. The peak starting at around 0 V vs Li^+/Li was related to the stripping of lithium. The liquid electrolyte-soaked PI nonwovens showed very excellent lithium deposition-stripping performance with high coulombic efficiency (95.7%) at high temperature. This high oxidative potential above 4.5 V and excellent lithium deposition-stripping performance at low potential would imply long-term reversibility of the cell chemistry at high temperature.

3.3. Ionic conductivity of the electrolyte-soaked PI nonwoven separator at high temperature

Fig. 5 presented the Nyquist plots of the electrochemical impedance for the liquid electrolyte-soaked PI nonwoven at 25 °C and 120 °C, respectively. It could be seen that the imaginary part of impedances were proportion to their real part at the low frequency range. The straight line with an angle meant a Warburg diffusion process. And the resistance of the electrolyte soaked nonwoven can be determined by the intersection of linear relation between the imaginary and real parts of the impedance with the real part axis. The ionic conductivity of the liquid electrolyte-soaked PI-5 nonwoven was calculated to be 0.89 mS cm^{-1} at 25 °C and 1.73 mS cm^{-1} at 120 °C respectively, which reached the acceptable order of 10^{-3} S cm^{-1} at high temperature [30–32]. So, it was verified that this liquid electrolyte-soaked PI nonwoven exhibited considerable ionic conductivity in 0.5 M LiBOB/PC electrolyte.

3.4. Battery performance of the electrolyte-soaked PI nonwoven separator at high temperature

Fig. 6(a) depicts a comparison of the charge–discharge curves at 0.5 *C* rate for the test cells using the PI nonwoven and the Celgard membrane at 80 °C. Both cells using the PI-5 nonwoven and the

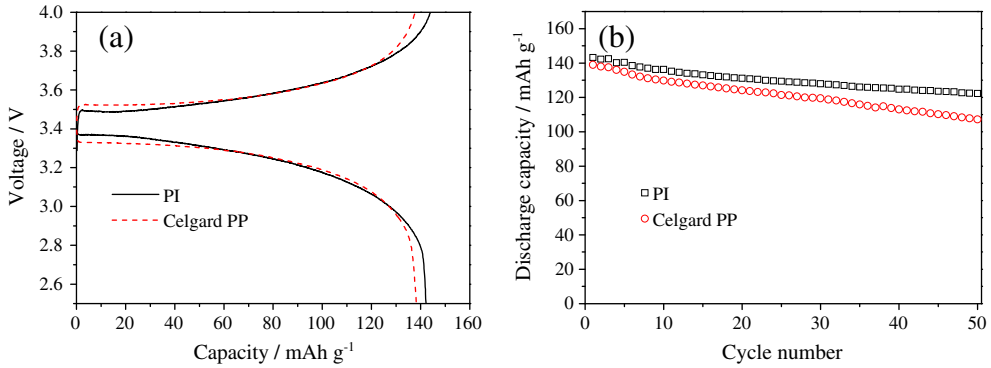

Fig. 6. (a) Charge–discharge curves for the cells using the PP membrane and the PI nonwoven at 0.5 *C* rate at 80 °C; (b) Discharge capabilities *vs.* cycle number of the cells using the PP membrane and the PI nonwovens at 80 °C.

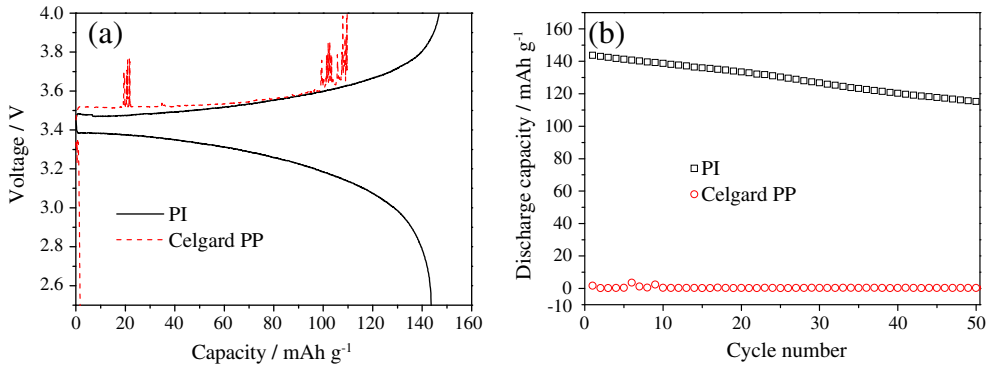

Fig. 7. (a) Charge–discharge curves for the cells using the PP membrane and the PI nonwoven at 0.5 *C* rate at 120 °C. (b) Discharge capabilities *vs.* cycle number of the cells using the PP membrane and the PI nonwovens at 120 °C.

Celgard membrane showed stable charge–discharge curves with discharge capacity of about 142 $mAhg^{-1}$ and 138 $mAhg^{-1}$, respectively. Cycle stabilities of the cells using the PI nonwoven and the Celgard membrane were displayed in Fig. 6(b) at charge/discharge rate of 0.5 C. The coulumbic efficiency of each cycle was maintained to be about 98%. The obtained discharge capacities after 50 cycles were kept around 130 $mAhg^{-1}$ and 110 $mAhg^{-1}$, indicative of capacity retention ratios at around 91% and 80% respectively, which meant both PI nonwoven and the Celgard membrane exhibited comparable cycling performance at 80 °C.

Fig. 7(a) depicts a comparison of the charge–discharge curves at 0.5 *C* rate for the test cells using the Celgard membrane and the PI nonwoven at 120 °C. Unfortunately, the cell using the PP membrane could not even be stably charged to 4.0 V for the first cycle. This might be due to the thermal shrinkage of the micropores at high temperature of 120 °C. The cells using the PI nonwoven showed stable charge–discharge curves with discharge capacity of about 142 $mAhg^{-1}$ with initial coulumbic efficiency of 97.8%. The stable voltage profiles at 120 °C would be ascribed to the excellent thermal stability and electrochemical stability of PI nonwoven. Cycle stabilities of the cells with PI nonwoven were displayed in Fig. 7(b) at charge/discharge rate of 0.5 C. The obtained discharge capacities after 50 cycles were kept around 120 $mAhg^{-1}$ indicative of capacity retention ratios at around 86%. These results demonstrated that PI nonwoven exhibited excellent charge–discharge performance and cyclability at high temperature of 120 °C.

4. Conclusions

The thermosetting polyimide nanofiber based nonwovens showed no thermal shrinkage at 150 °C and considerable mechanical strength compared to the Celgard PP membrane owing to the high temperature resistance of imide structure and the physical bonding between the nano fibers. Moreover, the LiBOB/PC soaked PI nonwovens possess high oxidative potential above 4.5 V and considerable ionic conductivity at high temperature of 120 °C The cells using LiBOB/PC soaked polyimide nonwovens as separator exhibited stable charge–discharge profiles and satisfactory cyclability at this high temperature. The superior electrochemical performance at high temperature could make these polyimide nonwovens an alternative to PP separators for high power or high temperature application.

Acknowledgments

This work was supported by the Instrument Developing Project of the Chinese Academy of Sciences (no. YZ201137), the National Program on Key Basic Research Project of China (973 Program) (no. MOST2011CB935700), the National Natural Science Foundation (nos. 20971077 and 20902052), Shangdong Province Fund for Distinguished Young Scientist (no. JQ200906) and Natural Science (no. ZR2009BM014).

Appendix A. Supplementary data

Supplementary data to this article can be found online at http://dx.doi.org/10.1016/j.ssi.2012.11.010.

References

[1] P. Arora, Z.G. Zhang, Chem. Rev. 104 (2004) 4419.
[2] S.S. Zhang, J. Power Sources 164 (2007) 351.
[3] J. Hassoun, S. Panero, B. Scrosati, J. Mater. Chem. 17 (2007) 3668.
[4] H. Li, Z.X. Wang, L.Q. Chen, X.J. Huang, Adv. Mater. 21 (2009) 4593.
[5] M.R. Palacin, Chem. Soc. Rev. 21 (2009) 4593.
[6] T.H. Cho, T. Sakai, S. Tanase, K. Kimura, Y. Kondo, T. Tarao, M. Tanaka, Electrochem. Solid-State Lett. 10 (2007) A159.
[7] D. Djian, F. Alloin, S. Martinet, H. Lignier, J.Y. Sanchez, J. Power Sources 172 (2007) 416.
[8] T.H. Cho, M. Tanaka, H. Onishi, Y. Kondo, T. Nakamura, H. Yamazaki, S. Tanase, T. Sakai, J. Power Sources 181 (2008) 155.
[9] T.H. Cho, M. Tanaka, H. Onishi, Y. Kondo, T. Nakamura, H. Yamazaki, S. Tanase, T. Sakaia, J. Electrochem. Soc. 155 (2008) A699.
[10] S.H. Yoo, C.K. Ki, Ind. Eng. Chem. Res. 48 (2009) 9936.
[11] Y.S. Chung, S.H. Yoo, C.K. Kim, Ind. Eng. Chem. Res. 48 (2009) 4346.
[12] S.J. Gwon, J.H. Choi, J.Y. Sohn, Y.M. Lim, Y.C. Nho, Y.E. Ih, J. Ind. Eng. Chem. 15 (2009) 748.
[13] H. Yoneda, Y. Nishimura, Y. Doi, M. Fukuda, M. Kohno, Polym. J. 42 (2010) 425.
[14] J.Y. Kim, D.Y. Lim, Energies 3 (2010) 866.
[15] M. Kim, J.Y. Shon, Y.C. Nho, T.W. Lee, J.H. Parka, J. Electrochem. Soc. 157 (2010) A31.
[16] G. Jeong, Y.U. Kim, H. Kim, Y.J. Kim, H.J. Sohn, Energy Environ. Sci. 4 (2011) 1986.
[17] B. Scrosati, J. Hassoun, Y.K. Sun, Energy Environ. Sci. 4 (2011) 3287.
[18] S. Mestre-Aizpuruaa, S. Hameletb, C. Masquelierb, M.R. Palacína, J. Power Sources 195 (2010) 6897–6901.
[19] H.S. Jeong, J.H. Kim, S.Y. Lee, J. Mater. Chem. 20 (2010) 9180.
[20] J.H. Cho, J.H. Park, J.H. Kim, S.Y. Lee, J. Mater. Chem. 21 (2011) 8192.
[21] E.S. Choi, S.Y. Lee, J. Mater. Chem. 21 (2011) 14747.
[22] Z.H. Liu, W. Jiang, Q.S. Kong, C.J. Zhang, P.X. Han, X.J. Wang, J.H. Yao, G.L. Cui, Macromol. Mater. Eng. (2012), http://dx.doi.org/10.1002/mame.201200158.
[23] D. Bansal, B. Meyer, M. Salomon, J. Power Sources 178 (2008) 848.
[24] C.B. Huang, S.Q. Wang, H.A. Zhang, T.T. Li, S.L. Chen, C.L. Lai, H.Q. Hou, Eur. Polym. J. 42 (2006) 1099.
[25] K. Amine, J. Liu, I. Belharouak, Electrochem. Commun. 7 (2005) 669–673.
[26] J. Jiang, J.R. Dahn, Electrochem. Commun. 6 (2004) 39–43.
[27] K. Xu, S.S. Zhang, T.R. Jow, W. Xu, C.A. Angell, Electrochem. Solid-State Lett. 5 (2002) A26–A29.
[28] M.M. Rao, X.Y. Geng, Y.H. Liao, S.J. Hua, W.S. Li, J. Membr. Sci. 399–400 (2012) 37–42.
[29] J.J. Miao, M. Miyauchi, T.J. Simmons, J.S. Dordick, R.J. Linhardt, J. Nanosci. Nanotechnol. 10 (2010) 55.
[30] N. Kaskhedikar, G.L. Cui, J. Maier, J. Mater. Chem. 21 (2011) 11838.
[31] X.L. Wu, S. Xin, H.H. Seo, J. Kim, Y.G. Guo, J.S. Lee, Solid State Ionics 186 (2011) 1.
[32] B. Xie, L.F. Li, H. Li, L.Q. Chen, Solid State Ionics 180 (2009) 688.